



Novel Fe (III) heterochelates: Synthesis, structural features and fluorescence studies

C.K. Modi^{a,*}, D.H. Jani^b, H.S. Patel^b, H.M. Pandya^a

^a Department of Chemistry, Bhavnagar University, Old Campus, Bhavnagar 364 002, Gujarat, India

^b Department of Chemistry, Sardar Patel University, Vallabh Vidyanagar 388 120, Gujarat India

ARTICLE INFO

Article history:

Received 21 July 2009

Received in revised form

19 December 2009

Accepted 31 December 2009

Keywords:

Fe (III) heterochelates

4-Acyl pyrazolone based hydrazides

Quinolone based drug

Fluorescence studies

ABSTRACT

Fluorescence properties of five 4-acyl pyrazolone based hydrazides (H_2SB_n) and their Fe (III) heterochelates of the type $[Fe(SB_n)(L)(H_2O)] \cdot mH_2O$ [H_2SB_n = nicotinic acid [1-(3-methyl-5-oxo-1-phenyl-4,5-di hydro-1H-pyrazol-4yl)-acylidene]-hydrazide; where acyl = $-CH_3$, $m=4$ (H_2SB_1); $-C_6H_5$, $m=2$ (H_2SB_2); $-CH_2-CH_3$, $m=3$ (H_2SB_3); $-CH_2-CH_2-CH_3$, $m=1.5$ (H_2SB_4); $-CH_2-C_6H_5$, $m=1.5$ (H_2SB_5) and HL = 1-cyclopropyl-6-fluoro-4-oxo-7-(piperazin-1-yl)-1,4-dihydroquinoline-3-carboxylic acid] were studied at room temperature. The fluorescence spectra of heterochelates show red shift, which may be due to the chelation by the ligands to the metal ion. It enhances ligand ability to accept electrons and decreases the electron transition energy. The kinetic parameters such as order of reaction (n), energy of activation (E_a), entropy (S^*), pre-exponential factor (A), enthalpy (H^*) and Gibbs free energy (G^*) have been reported.

© 2010 Elsevier B.V. All rights reserved.

1. Introduction

Fluorescent compounds have potential applications as fluorescent sensor molecules in their solution for research in biology and environmental science [1–7]. In the development of new luminescent materials, metal complexes with Schiff base ligands are very important for their applications.

4-Acyl pyrazolones can form a variety of Schiff bases and are reported to be superior reagents in biological, clinical and analytical applications [8] variety of coordination compounds due to keto–enol tautomerism in them [9]. Compounds containing hydrazide and acylhydrazone moieties and their complexes also possess biological activities, especially as potential inhibitors for many enzymes [10,11].

Previously, we have synthesized a series of 4-acyl pyrazolone derivatives and their transition metal complexes [12–14]. However, no information is available on their fluorescence properties. Hence, in this paper, we report fluorescence properties of some 4-acyl pyrazolone derivatives and their Fe (III) heterochelates. The suggested structure of Schiff base ligands (H_2SB_n) is shown in Scheme 1.

2. Experimental

2.1. Materials

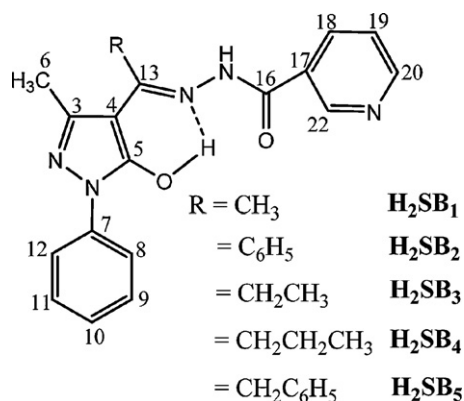
All the chemicals used were of analytical grade and used without further purification. The compounds 1-phenyl-3-methyl-2-pyrazoline-5-ol and β -picolinic hydrazide were purchased from E. Merck Ltd. (India). Acyl chlorides were purchased from Qualigens Fine Chemicals, India and used without further purification. Quinolone based drug (HL) was purchased from Bayer AG (Wuppertal, Germany).

2.2. Instruments

The fluorescence behaviors of ligands and their Fe (III) heterochelates were studied using a Shimadzu RF-1501 Fluorescence Spectrophotometer with Xe arc lamp as the light source at room temperature. The slit width for excitation and emission was 10 nm, and the scan speed was 1200 nm/min. Elemental analyses (C, H, N) were carried out on Perkin–Elmer, USA, 2400-II CHN analyzer. FT-IR spectra were recorded as KBr pellets on Nicolet-400D spectrophotometer. 1H NMR spectra were recorded on Advance 400 Bruker FT-NMR instrument in $DMSO-d_6$ solvent. The magnetic moments were obtained by the Gouy's method using mercury tetrathiocyanato cobaltate (II) as a celebrant ($g = 16.44 \times 10^{-6}$ c.g.s. units at 20 °C). The FAB-mass spectrum of the heterochelate was recorded with JEOL SX-102/DA-6000 mass spectrometer. Simultaneous TG/DTGs were obtained by a model 5000/2960 SDT, TA Instruments, USA. The experiments were performed in N_2 atmo-

* Corresponding author. Tel.: +91 278 2439852; fax: +91 278 2426706.

E-mail address: chetank.modi1@gmail.com (C.K. Modi).



Scheme 1. The structure of Schiff base ligands (H_2SB_n).

sphere at a heating rate of $10^\circ\text{C min}^{-1}$ in the temperature range $50\text{--}800^\circ\text{C}$, using Al_2O_3 crucible. DSCs were recorded using DSC 2920, TA Instrument, USA.

2.3. Synthesis of ligands [H_2SB_n (where $n = 1\text{--}5$): general procedure

Equimolar (10 mmol) ethanolic solutions (50 mL) of 3-methyl-1-phenyl-4-acyl-1H-pyrazol-5-one and β -picolinic acid hydrazide (25 mL) were refluxed with stirring for 3 h in round bottom flask. The resulting solution was cooled overnight at room temperature in an evaporating dish. The solvent was removed by evaporation and colored oily product was obtained which was washed with diethyl ether and dried in vacuo to constant mass and finally purified by crystallized in appropriate solvents.

2.4. Synthesis of heterochelates

The preparation of heterochelates was carried out by mixing hot methanolic solution (50 mL) of $\text{Fe}(\text{NO}_3)_3 \cdot 9\text{H}_2\text{O}$ (10 mmol) and a hot methanolic solution (50 mL) of the Schiff base (H_2SB_n) (10 mmol) and HL ligand (10 mmol) in water. The pH was adjusted to 6–7 by drop wise addition of 25% NaOH solution in water. The mixture was heated in a water bath for 4 h at 60°C . The mixture was kept overnight at room temperature. The obtained colored crystals were washed with water, methanol and finally with diethyl ether and dried in air.

3. Results and discussion

The analytical and physical data of the Schiff base ligands (H_2SB_n) and their heterochelates are shown in [Supplemental Data](#). The heterochelates are colored and stable in air. They are insoluble in water and in most organic solvents but soluble in DMF. The formation of the heterochelates is assumed according to the chemical reaction as shown below:



(where $n = 1, m = 4$; $n = 2, m = 2$; $n = 3, m = 3$; $n = 4$ and $5, m = 1.5$)

3.1. IR spectra of H_2SB_n and their heterochelates

The important infrared spectral bands and their tentative assignments for the synthesized ligands and their heterochelates were recorded as KBr disks. The Schiff base ligands H_2SB_n (where $n = 1\text{--}5$) in the present investigation exhibit a broad band centered at $3372\text{--}3395\text{ cm}^{-1}$. This suggests the presence of a strongly

hydrogen-bonded --OH group. This indicates the involvement of the 5-OH group in intramolecular hydrogen bonding with azomethine nitrogen. It also suggests that the ligands exist in enol form in the solid state [15].

The Schiff base ligands (H_2SB_n) contain five potential donor sites: (i) the enolic oxygen of the 5-OH group; (ii) the acyclic azomethine nitrogen; (iii) amide nitrogen of amide-imidol form of hydrazone moiety and (iv) carbonyl oxygen of amide-imidol form of hydrazone moiety.

The Schiff base ligands (H_2SB_n) show a sharp and strong band due to $\nu_{(\text{C}=\text{N})}$ of the acyclic azomethine group at $1630\text{--}1640\text{ cm}^{-1}$. The observed low-energy shift of this band in the heterochelates at $1608\text{--}1620\text{ cm}^{-1}$ suggests the coordination of azomethine nitrogen [16].

The $\nu_{(\text{N-H})}$ and $\nu_{(\text{C}=\text{O})}$ modes of the lateral chain in the free Schiff bases appear at $3170\text{--}3192$ and $1690\text{--}1702\text{ cm}^{-1}$, respectively, indicates that the ligands exist in keto form in solid state. However, in solution, ligands probably exist in tautomeric enol form. The infrared spectra of heterochelates show a considerable negative shift of $10\text{--}15\text{ cm}^{-1}$ in $\nu_{(\text{C}=\text{O})}$ absorption of the pyrazolone group, indicating a decrease in the stretching force constant of $(\text{C}=\text{O})$ as a consequence of coordination through the oxygen atom of the ligand. Meanwhile, the new absorption band attributed to $\nu_{(\text{C}=\text{O})}$ [17] was observed at $1325\text{--}1333\text{ cm}^{-1}$. From these observations, it is concluded that the ligand reacts in enol form with prototropy, which incorporates into proton transfer through oxygen atom of the ligand forming two bonds with the metal ion.

In the present heterochelates, the bands observed in the region $3420\text{--}3440$, $1278\text{--}1298$, $850\text{--}880$ and $700\text{--}712\text{ cm}^{-1}$ are attributed to --OH stretching, bending, rocking and wagging vibrations, respectively due to the presence of water molecules. The presence of rocking band indicates the coordination nature of the water molecule [18].

Comparing the main IR frequencies of Fe (III) heterochelates with that of ciprofloxacin (HL) ligand, the following results were found. Two very strong absorption peaks in the spectrum of the ligand were observed at 1707 and 1627 cm^{-1} due to $\nu(\text{O-H})$ of the carboxylic group and $\nu(\text{C}=\text{O})$ groups, respectively. Absence of the former band in the spectra of the heterochelates suggests that this moiety participated in the bonding to the metal ion [19]. The latter band corresponding to $\nu(\text{C}=\text{O})$ shifted to the lower frequency region ($\sim 1620\text{ cm}^{-1}$) in the spectra of the heterochelates could be, due to coordination through either the ketone group or the carboxylic group, to the metal ion. We confirm that the coordination was through the ketonic group of the HL ligand as the antisymmetric $\nu_{\text{as}(\text{COO}^-)}$ and symmetric $\nu_{\text{s}(\text{COO}^-)}$ modes of the carboxylate group were observed at 1620 and 1384 cm^{-1} , respectively. The heterochelates produced a $\Delta\nu$ value of $>200\text{ cm}^{-1}$ in $\nu_{\text{as}(\text{COO}^-)}$ ($1595\text{--}1588\text{ cm}^{-1}$) and $\nu_{\text{s}(\text{COO}^-)}$ ($1380\text{--}1370\text{ cm}^{-1}$) suggesting unidentate carboxylate coordination to the central metal ions [12,20–22]. Accordingly ciprofloxacin (HL), in the isolated heterochelates appears to act as a uninegative bidentate ligand through the oxygen atom of the carbonyl group and enolic oxygen of the carboxylic group.

In the far-IR region, two new bands at $455\text{--}465$ and $410\text{--}420\text{ cm}^{-1}$ in the heterochelates are assigned to $\nu_{(\text{M-O})}$ pyrazolone and $\nu_{(\text{M-N})}$ modes, respectively. All of these data confirm the fact that H_2SB_n behaves as a dinegative tridentate ligand forming a conjugated chelate ring, with the ligand existing in the heterochelates in the enolized form.

3.2. $^1\text{H NMR}$ spectra of H_2SB_n and their heterochelates

The tautomerism of pyrazolones is an old problem of pyrazole chemistry and thus it has been the subject of a considerable num-

ber of studies [23–28]. The ^1H NMR studies of Schiff base ligands (H_2SB_n) (where $n = 1-5$) and their heterochelates were carried out in $\text{DMSO}-d_6$ at room temperature. A broad singlet corresponding to one proton for Schiff base ligands (H_2SB_n) is observed in the range δ 11.9–12.7 ppm. This signal disappeared when D_2O exchange experiment was carried out. It shows the enolic nature of ligand and broadness of singlet due to fast exchange interaction of proton via keto–enol tautomerism with nitrogen of the azomethine group [29]. It may be noted that the integration of this signal perfectly matches with one proton and there is no other fragment(s) of this signal, which suggests that only one tautomeric form of the Schiff base ligands exists in solution under the experimental conditions. Comparing with the solid state study, we prefer to assign this signal to OH; however, assignment of this peak to NH cannot be ruled out provided solid state structural evidence is not considered.

In the aromatic region, specifically for H_2SB_2 ligand, phenyl protons of the benzoyl group indicate the typical effect on their chemical shifts, whose signals are observed in the down field region from the benzene standard ($\delta = 7.01-7.58$) in the order of *ortho*-, *para*-, and *meta*-positions ($\Delta\delta = \text{positive } o \gg p > m$) characteristic for a monosubstituted benzene bonded to the electrophilic $>\text{C}=\text{N}$ group (chemical shift values (δ) *o*: 7.83, *m*: 7.64 and *p*: 7.60 ppm of Ph-ring protons of 4-benzoyl group). On the other hand, phenyl protons bonded to the N atom of the pyrazolone ring show a net effect of the diamagnetic ring current on the pyrazolone ring and the electron-donating property of the $>\text{N}=\text{N}$ group (chemical shift values (δ) *o*: 7.58, *m*: 7.26 and *p*: 7.11 ppm of Ph-ring protons of pyrazolone group). Both of these effects further increase aromaticity of the pyrazolone ring due to the electron delocalization on the ring system. It should be noted that the ring current effect is a down field shift ($\Delta\delta = \text{positive } o \gg p > m$), while the electron-donating effect is an up field shift ($\Delta\delta = \text{negative } m \gg p > o$) [30]. Probably, the ring current effect is much greater than the electron-donating one, and thus we get the order of chemical shift values (δ) *o*: 7.62, *m*: 7.20 and *p*: 7.04 for the heterochelates.

It was found that the signal of the $-\text{NH}$ proton of the lateral chain of Schiff bases (H_2SB_n) disappeared in the spectra of heterochelates, presumably because of enolization and subsequent loss of $-\text{NH}$ proton by coordination with the metal ion through carbonyl oxygen.

In the ^1H NMR spectra of Schiff bases (H_2SB_n), the pyridine ring ($\text{C}_5\text{H}_4\text{N}$) protons appeared as multiplet in the region of δ 7.98–9.10 ppm [31,32], which remain unaltered in the spectra of heterochelates suggesting non-involvement of this group in coordination.

3.3. Mass spectra

The representative mass spectrum of the Schiff base H_2SB_2 ligand is shown in Supplemental Data. The molecular ion peak was observed at m/e 397 (Calcd. 397.15). A weak peak at m/e 277 (Calcd. 276.11) is due to the formation of $(\text{C}_{17}\text{H}_{14}\text{N}_3\text{O})^+$, with the elimination of one $-\text{NH}$ group and $(\text{C}_6\text{H}_4\text{NO})^+$ m/e 106 (Calcd. 106.03) ion from the molecule. The species further degrade with the loss of one $-\text{CH}_3$ group forming $(\text{C}_{16}\text{H}_{11}\text{N}_3\text{O})^+$ with peak at m/e 261 (Calcd. 261.09). Prominent peaks for $(\text{C}_6\text{H}_5\text{N})^+$ and $(\text{C}_6\text{H}_5)^+$ ions are observed at m/e 91 and 77, respectively.

The recorded mass spectra (Fig. 1) and the molecular ion peak for the heterochelate $[\text{Fe}(\text{SB}_1)(\text{L})(\text{H}_2\text{O})]\cdot 4\text{H}_2\text{O}$ have been used to confirm the molecular formulae. The first peak at m/e 736 represents the molecular ion peak of the heterochelate. The fragmentation pattern is given in Scheme 2. The primary fragmentation of the heterochelate takes place due to the loss of $-\text{CH}_3$ group from the species (a) to give species (b) with peak at m/e 723. The species (b) further degrades with the subsequent loss of one coordinated water molecule and $-\text{C}_3\text{H}_5$ species forming species (c) with their peak at m/e 662. The sharp peak (base peak) observed at m/e 390 represents the stable species (g) with 99.6% abundance.

3.4. Fluorescence spectra of ligands [H_2SB_n] (where $n = 1-5$) and its heterochelates

The liquid-state fluorescence emission spectra of the ligands (H_2SB_n) and its heterochelates were measured in *N,N*-dimethyl formamide (DMF) with a concentration of 1×10^{-5} M at room temperature. The fluorescence emission spectra of ligands (H_2SB_n) and their heterochelates are displayed in Figs. 2 and 3, respectively. Obviously, upon excitation at $\lambda_{\text{max,ex}} = 550$ nm, all the ligands [H_2SB_n] (where $n = 1-5$) exhibit fluorescent properties in the green

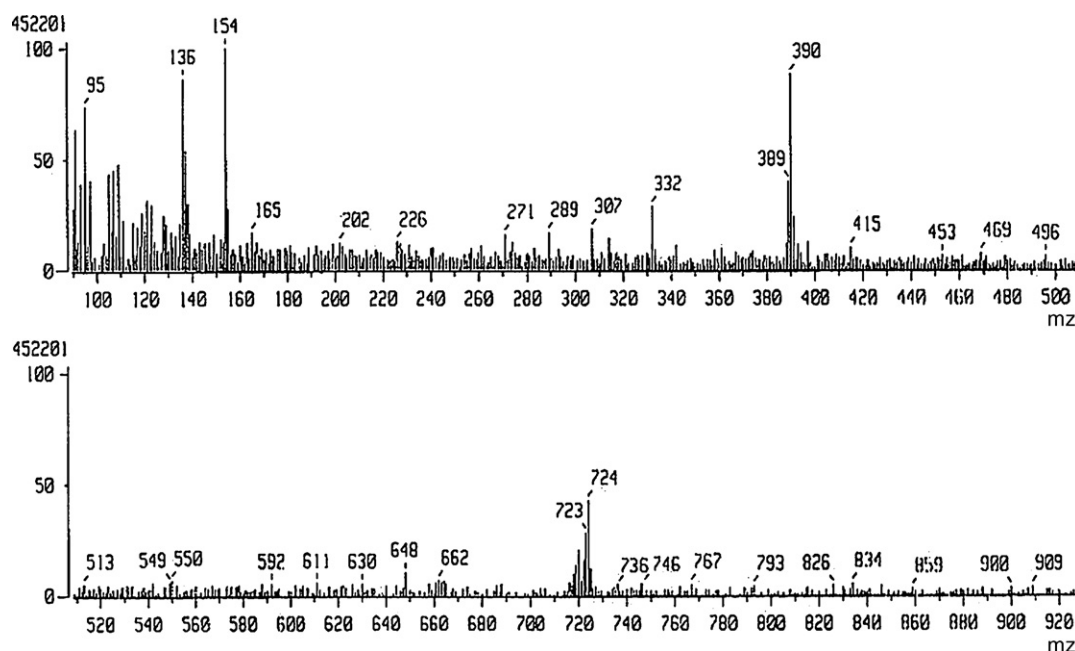
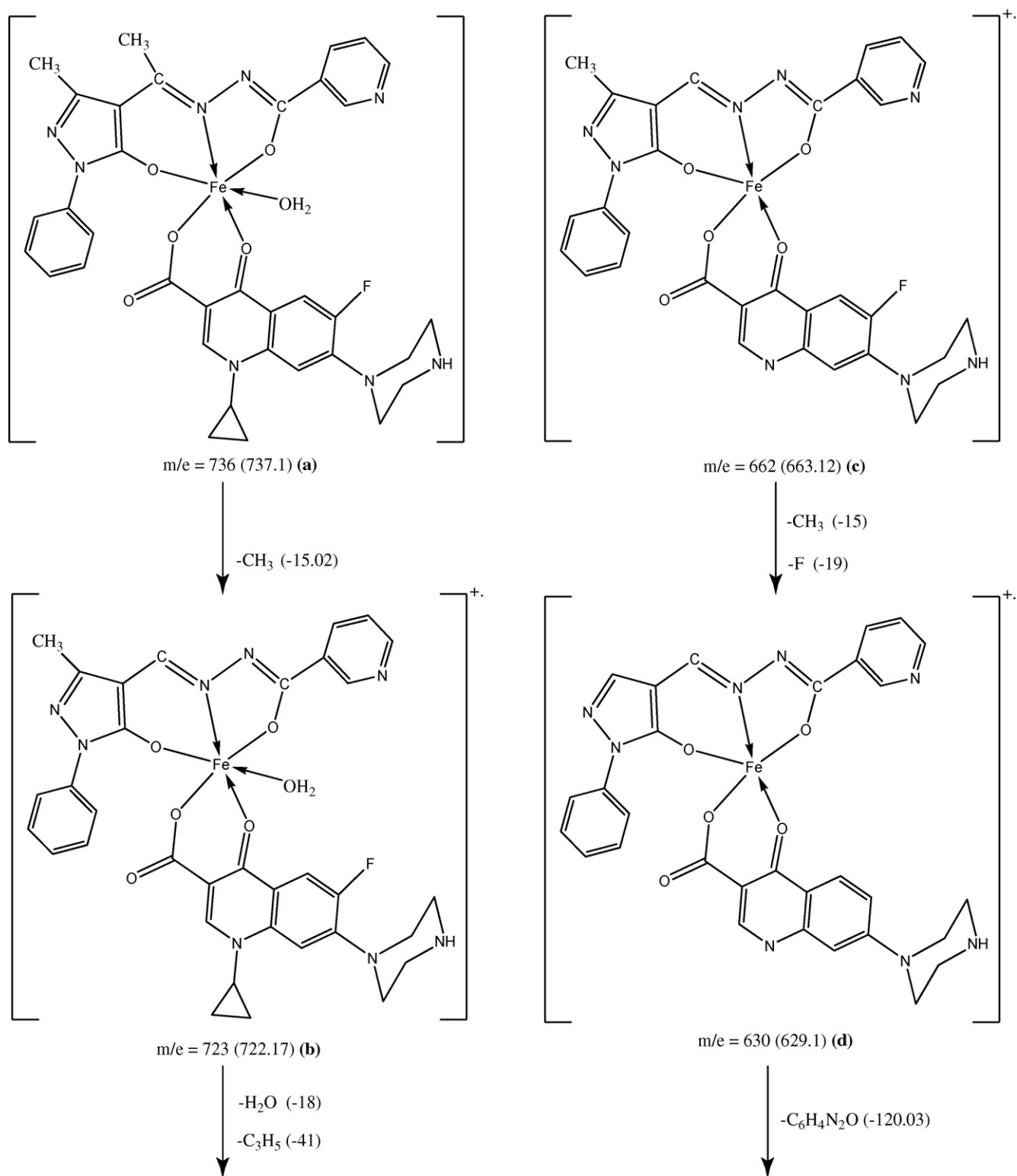


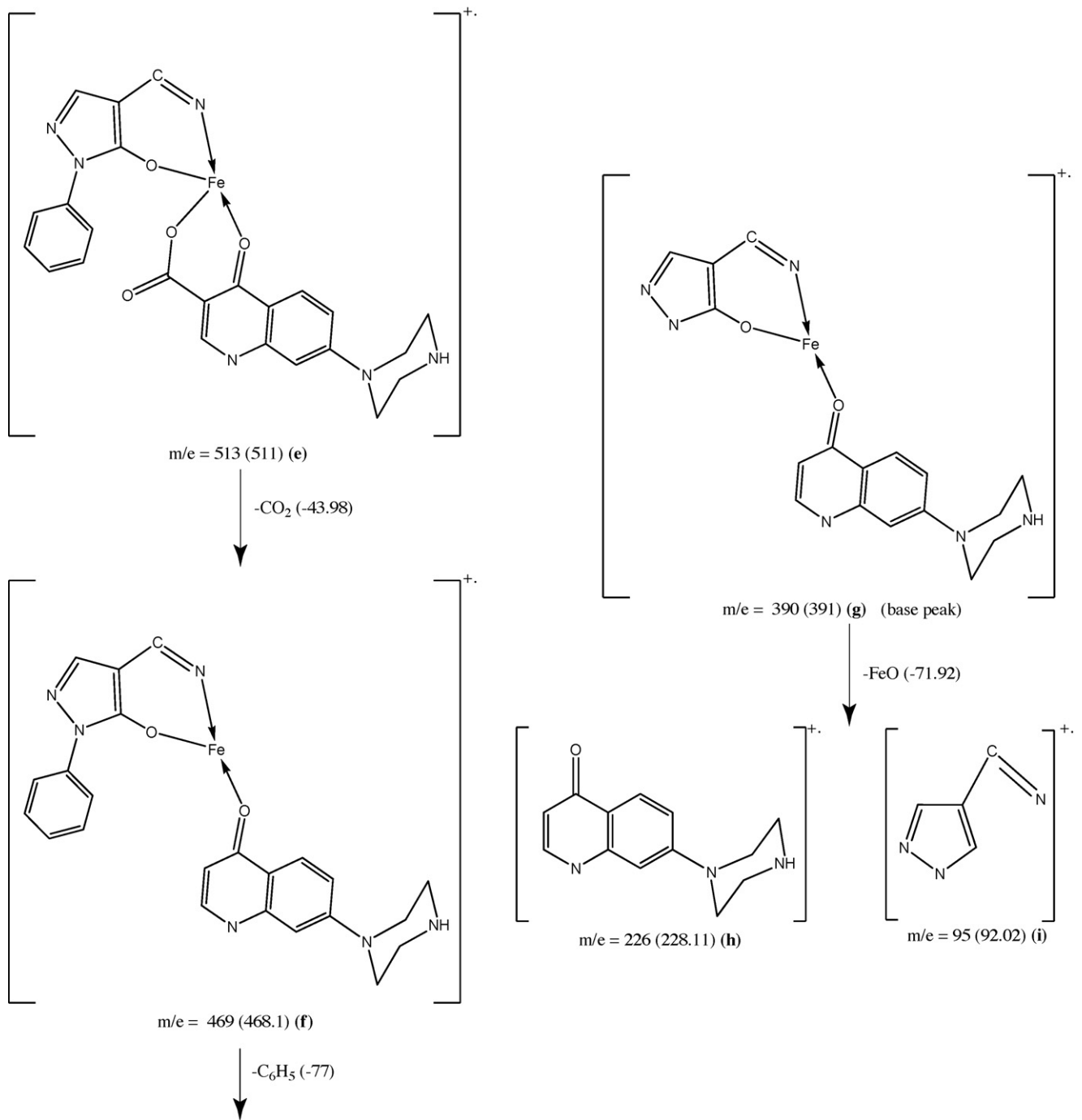
Fig. 1. The typical FAB-mass spectrum of a heterochelate $[\text{Fe}(\text{SB}_1)(\text{L})(\text{H}_2\text{O})]\cdot 4\text{H}_2\text{O}$.

region at room temperature, and the maximum emission peaks are at 615, 620, 620, 625 and 700 nm, respectively. There are slight red shifts of the emission energies of the five ligands. Moreover, the fluorescence emission intensities depend upon the introduction of different substitutions in the ligand molecules. Electro-donating groups (propyl, ethyl and methyl) and electro-withdrawing groups (phenyl, benzyl) on the 4-position of the pyrazolone ring can

drastically alter the electron density and the electron conjugate system of the ligands H_2SB_n [33,34]. However, when the heterochelates are excited at the same wavelength, the spectra of the heterochelates $[Fe(SB_n)(L)(H_2O)] \cdot mH_2O$ (where $n = 1-5$) have a slightly red shift as compared to the ligands as shown in Fig. 3, which probably was led by the charge transfer that was caused by the alternation of the structure of the ligand during the formu-



Scheme 2. The suggested fragmentation pattern of $[Fe(SB_1)(L)H_2O] \cdot 4H_2O$.



Scheme 2. (Continued).

lation of heterochelate. The maximum emission of heterochelate $[\text{Fe}(\text{SB}_4(\text{L})(\text{H}_2\text{O})) \cdot 1.5\text{H}_2\text{O}]$ is at 455 nm in the blue region, while those of $[\text{Fe}(\text{SB}_5(\text{L})(\text{H}_2\text{O})) \cdot 1.5\text{H}_2\text{O}]$ heterochelate with maximum emission band at 800 nm in the red region. Except for the emission intensity, the shapes of the emission spectra of ligands H_2SB_n and their heterochelates are similar, so the emission properties of heterochelates are believed to originate from $\pi^* \rightarrow \pi$ transitions in the ligands. The significant red shift of the fluorescence spectra of the heterochelates compared to ligands may be due to the chelating of the ligand to the Fe (III) ion, which enhances the ligands ability to accept electrons and decreases the electron transition energy [35].

3.5. Electronic spectra and magnetic moments

The information regarding geometry of the heterochelates was obtained from their electronic spectral data and magnetic moment values. In the present work, electronic spectra of heterochelates exhibit two bands at around $\sim 20,000$ and $\sim 32,500 \text{ cm}^{-1}$ are assigned to the ${}^6\text{A}_{1g} \rightarrow {}^4\text{T}_{2g}$ and MLCT transitions, respectively in the d^5 -system of the Fe (III) atom. From the electronic spectra, an octahedral geometry around the central metal ion is suggested. This is further supported by the magnetic measurement data of Fe (III) heterochelates which falls in the range 5.90–6.01 B.M. [36,37].

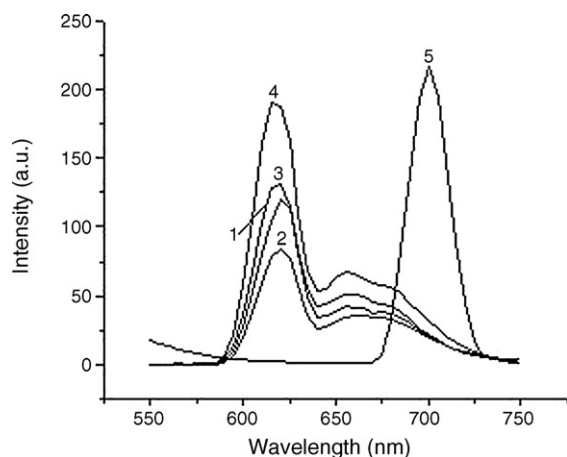


Fig. 2. Fluorescence spectra of ligands $[H_2SB_n]$ (where $n = 1-5$) in 10^{-5} M DMF solution at room temperature.

3.6. Thermal studies

Each decomposition process follows the trend



This process comprises of several stages. The method reported by Freeman–Carroll method [38] has been adopted. Plots of $[\Delta \log(dw/dt)/\Delta \log wr]$ vs. $[\Delta(1/T)/\Delta \log wr]$ were linear for all of the decomposition steps. The energy of activation E_a was calculated from the slopes of these plots for a particular stage and the order of reactions (n) determined from the intercept, showing first order reaction over the entire range of decomposition for all of the heterochelates. A typical Freeman–Carroll plot for the thermal degradation of $[Fe(SB_4)(L)H_2O] \cdot 1.5H_2O$ is shown in Fig. 4.

3.6.1. The thermal behavior of heterochelates

The thermal fragmentation scheme for heterochelates $[Fe(SB_n)(L)(H_2O)] \cdot mH_2O$ is as shown below:

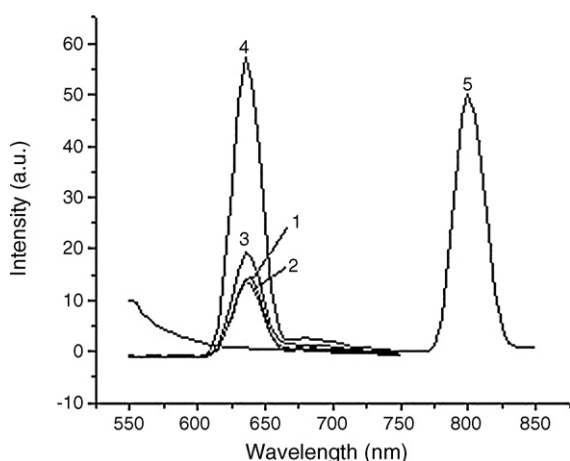
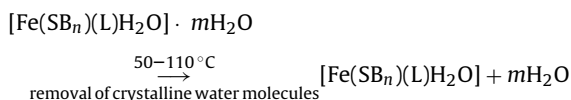


Fig. 3. Fluorescence spectra of heterochelates $[Fe(SB_n)(L)(H_2O)] \cdot mH_2O$ (where $n = 1-5$) in 10^{-5} M DMF solution at room temperature.

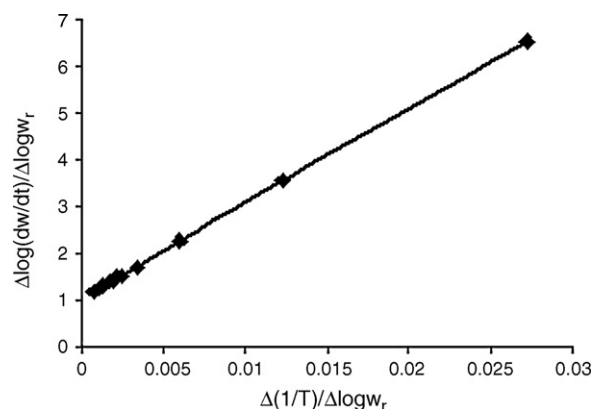
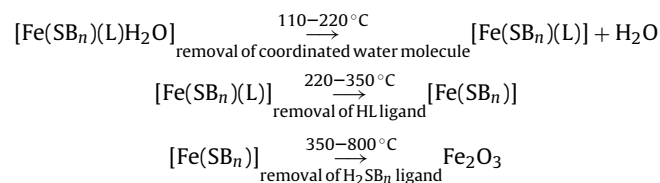
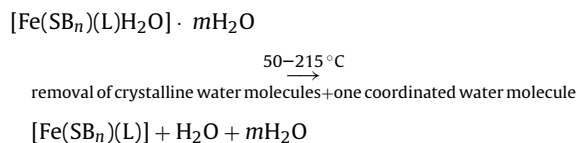


Fig. 4. The typical Freeman–Carroll plot for thermal degradation of a heterochelate $[Fe(SB_4)(L)(H_2O)] \cdot 1.5H_2O$.

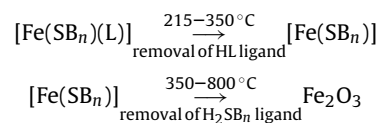
(where $n = 1, m = 4; n = 3, m = 3; n = 4, m = 1.5$)



Whereas the thermal fragmentation scheme for heterochelates $[Fe(SB_n)(L)(H_2O)] \cdot mH_2O$ (where $n = 2, m = 2; n = 4, m = 1.5$) is given below:



(where $n = 2, m = 2; n = 5, m = 1.5$)



The anhydrous heterochelates show great thermal stability up to $220^\circ C$; and in the third subsequent stage for heterochelates, the decomposition and combustion of ligand (HL) occurs, the fourth subsequent stage for heterochelates shows the decomposition and combustion of ligand (H_2SB_n). The removal of ligand (H_2SB_n) undergoes decomposition forming Fe_2O_3 as the final residue.

The thermodynamic activation parameters of the decomposition process of dehydrated heterochelates such as activation entropy (S^*), pre-exponential factor (A), activation enthalpy (H^*) and free energy of activation (G^*), were calculated using the reported equations [39] and are tabulated in Table 1. According to the kinetic data obtained from DTG curves, all the heterochelates have negative entropy, which indicates that the studied heterochelates have more ordered systems than reactants [40]. The kinetic parameters, especially energy of activation (E_a) is helpful in assigning the strength of the bonding of ligand moieties with the metal ion. The calculated E_a values of the investigated heterochelates for the degradation stage of ligand (HL) are in the range $25.25-32.54 \text{ kJ mol}^{-1}$. The relative high E_a value indicates that the ligand (HL) is strongly bonded to the metal ion [41]. From the above discussion an octahedral geometry of the heterochelates can tentatively be assumed as shown in Fig. 5.

Table 1
Kinetic parameters of heterochelates.

Compounds	TG range (°C)	E_a (kJ mol ⁻¹)	n	A (s ⁻¹)	S^* (J K ⁻¹ mol ⁻¹)	H^* (kJ mol ⁻¹)	G^* (kJ mol ⁻¹)
[Fe(SB ₁)(L)(H ₂ O)]·4H ₂ O	50–110	12.55	0.98	0.97	-100.98	9.66	43.69
	110–200	14.36	0.98	1.22	-100.22	10.01	61.66
	200–340	25.25	0.99	3.97	-99.73	11.03	73.55
	340–800	38.32	1.00	5.25	-98.66	28.31	97.90
[Fe(SB ₂)(L)(H ₂ O)]·2H ₂ O	50–215	14.73	0.99	1.18	-102.09	9.96	32.77
	215–330	27.67	1.00	2.34	-99.00	20.62	66.69
	330–800	43.52	1.00	5.45	-98.14	30.31	103.85
	50–115	10.28	1.00	0.32	-103.46	5.52	43.41
[Fe(SB ₃)(L)(H ₂ O)]·3H ₂ O	115–200	17.22	1.00	19.66	-100.30	7.42	62.99
	200–340	30.69	0.99	22.42	-96.93	15.77	70.61
	340–800	33.84	0.98	33.55	-95.22	25.10	90.33
	50–90	9.21	1.01	0.11	-102.53	0.45	34.59
[Fe(SB ₄)(L)(H ₂ O)]·1.5H ₂ O	90–220	14.09	0.98	0.13	-101.51	2.49	58.63
	220–450	25.52	1.00	4.33	-97.31	11.51	78.45
	450–800	33.79	1.01	8.38	-96.22	26.95	107.04
	50–210	15.20	1.00	0.10	-102.52	0.47	35.54
[Fe(SB ₅)(L)(H ₂ O)]·1.5H ₂ O	210–350	32.54	0.99	2.20	-98.56	10.85	62.40
	350–800	41.31	1.01	33.55	-95.44	22.43	93.49

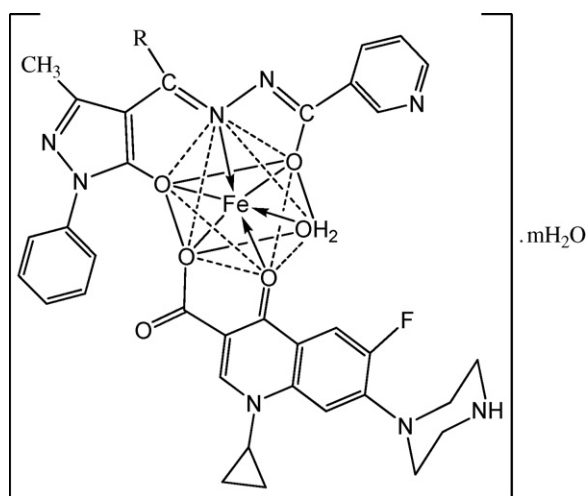


Fig. 5. The suggested structure of heterochelates.

4. Conclusions

The results obtained in this study allow the following conclusions:

1. Comparative fluorescence studies of 4-acyl pyrazolone based hydrazides [H₂SB_n] (where $n = 1-5$) and their Fe (III) heterochelates in the solution state have been done. The fluorescence spectra of the heterochelates show red shift, which may be due to the chelating of the ligands to the metal ion. It enhances ligand ability to accept electrons and decreases the electron transition energy.
2. The information regarding geometry of the heterochelates was obtained from their magnetic moment values. Magnetic moment values indicate that Fe (III) heterochelates are high spin, lacking exchange interactions. The study reveals that an octahedral geometry around the central metal ion as shown in Fig. 5.

Acknowledgements

We express our gratitude to the Head, Department of Chemistry, Sardar Patel University, Vallabh Vidyanagar, Gujarat, India for providing necessary laboratory facilities.

Appendix A. Supplementary data

Supplementary data associated with this article can be found, in the online version, at doi:10.1016/j.saa.2009.12.076.

References

- [1] S.C. Burdette, C.J. Frederickson, W.M. Bu, S.J. Lippard, *J. Am. Chem. Soc.* 125 (2003) 1778–1787.
- [2] Z.C. Xu, Y. Xiao, X.H. Qian, J.N. Cui, D.W. Cui, *Org. Lett.* 7 (2005) 889–892.
- [3] S. Banthia, A. Samanta, *J. Phys. Chem. B* 110 (2006) 6437–6440.
- [4] S. Mizukami, H. Houjou, K. Sugaya, E. Koyama, H. Tokuhisa, T. Sasaki, M. Kanetsato, *Chem. Mater.* 17 (2005) 50–56.
- [5] J. Li, L. Zhang, L. Liu, G. Liu, D. Jia, G. Xu, *Inorg. Chim. Acta* 360 (2007) 1995–2001.
- [6] S.J. Toal, K.A. Jones, D. Magde, W.C. Troglor, *J. Am. Chem. Soc.* 127 (2005) 11661–11665.
- [7] G.Q. Zhang, G.Q. Yang, L.N. Zhu, Q.Q. Chen, J.S. Ma, *Sens. Actuators B: Chem.* 114 (2006) 995–1000.
- [8] (a) M.F. Iskander, L. Sayed, A.F.M. Hefny, S.E. Zayan, *J. Inorg. Nucl. Chem.* 38 (1976) 2209–2216;
(b) H. Adams, D.E. Fenton, G. Minardi, E. Mura, M. Angelo, *Inorg. Chem. Commun.* 3 (2000) 24–28;
(c) Z.Y. Yang, R.D. Yang, F.S. Li, K.B. Yu, *Polyhedron* 19 (2000) 2599–2604.
- [9] J. Belmar, F.R. Pérezzb, J. Alderetea, C. Zúñigaa, *J. Braz. Chem. Soc.* 16 (2005) 179–189.
- [10] (a) N.L. Wengenack, S. Todorovic, L. Yu, F. Rusnak, *Biochemistry* 37 (1998) 15825–15834;
(b) N.L. Wengenack, H. Lopes, M.J. Kennedy, P. Tavares, A.S. Pereira, I. Moura, J.J.G. Moura, F. Rusnak, *Biochemistry* 39 (2000) 11508–11513.
- [11] (a) X.-B. Zhao, H. Yu, S.-W. Yu, F. Wang, J.C. Sacchettini, R.S. Magliozzo, *Biochemistry* 45 (2006) 4131–4140;
(b) A. Parenty, X. Moreau, J.-M. Campagne, *Chem. Rev.* 106 (2006) 911–939;
(c) A. Mai, S. Massa, R. Ragno, I. Cerbara, F. Jesacher, P. Loidl, G.J. Brosch, *Med. Chem.* 46 (2003) 512–524.
- [12] C.K. Modi, M.N. Patel, *J. Therm. Anal. Calorim.* 94 (1) (2008) 247–255.
- [13] C.K. Modi, I.A. Patel, B.T. Thaker, *J. Coord. Chem.* 61 (19) (2008) 3110–3121.
- [14] C.K. Modi, *Spectrochim. Acta A* 71 (2009) 1741–1748.
- [15] C.K. Modi, B.T. Thaker, *J. Therm. Anal. Calorim.* 94 (2) (2008) 567–577.
- [16] I.A. Patel, B.T. Thaker, *Ind. J. Chem.* 38A (1999) 427–433.
- [17] G. Xu, L. Liu, L. Zhang, G. Liu, D. Jia, J. Lang, *Struct. Chem.* 16 (4) (2005) 431–437.
- [18] N. Nakamoto, *Infrared Spectra and Raman Spectra of Inorganic and Coordination Compounds*, John Wiley & Sons, New York, 1978.
- [19] L.J. Bellamy, *The Infrared Spectra of Complex Molecules*, third ed., Chapman and Hall, London, 1975.
- [20] G.B. Deacon, R.J. Phillips, *Coord. Chem. Rev.* 33 (1980) 227–250.
- [21] B.S. Creaven, D.A. Egan, K. Kavanagh, M. McCann, A. Noble, B. Thati, M. Walsh, *Inorg. Chim. Acta* 359 (2006) 3976–3984.
- [22] M.S. Masoud, M.F. Amira, A.M. Ramadan, G.M. El-Ashry, *Spectrochim. Acta A* 69 (2008) 230–238.
- [23] F. Marchetti, C. Pettinari, R. Pettinari, *Coord. Chem. Rev.* 249 (2005) 2909–2945.
- [24] J.A.M. Guard, P.J. Steel, *Aust. J. Chem.* 47 (1994) 1453–1459.
- [25] A.A. Soliman, *Spectrochim. Acta A* 67 (2007) 852–857.
- [26] W. Holzer, K. Mereiter, B. Plagens, *Heterocycles* 50 (1999) 799–818.
- [27] Y. Akama, M. Shiro, T. Ueda, M. Kajitani, *Acta Cryst. C* 51 (1995) 1310–1314.
- [28] J. Elguero, C. Marzin, A.R. Katritzky, P. Linda, *Adv. Heterocycl. Chem.* 1 (1976) 313–336.

- [29] B.T. Thaker, K.R. Surati, S. Oswal, R.N. Jadeja, V.K. Gupta, *Struct. Chem.* 18 (2007) 295–310.
- [30] Y. Akama, T. Sawada, T. Ueda, *J. Mol. Struct.* 750 (2005) 44–50.
- [31] C.K. Modi, B.T. Thaker, *Ind. J. Chem.* 41A (2002) 2544–2547.
- [32] Z. Yang, R. Yang, Q. Li, *Synth. React. Inorg. Met. Org. Chem.* 29 (2) (1999) 205–214.
- [33] S. Mitra, S. Mukherjee, *J. Lumin.* 118 (2006) 1–11.
- [34] M. Fores, S. Scheiner, *Chem. Phys.* 246 (1999) 65–74.
- [35] J. Lu, L. Zhang, L. Liu, G. Liu, D. Jia, D. Wu, G. Xu, *Spectrochim. Acta A* 71 (3) (2008) 1036–1041.
- [36] A.B.P. Lever, *Inorganic Electronic Spectroscopy*, second ed., Elsevier, Amsterdam, 1984.
- [37] A.C. Massabni, P.P. Corbi, P. Melnikov, M.A. Zacharias, H.R. Rechenberg, *J. Coord. Chem.* 57 (2004) 1225–1231.
- [38] E.S. Freeman, B. Carroll, *J. Phys. Chem.* 62 (1958) 394–397.
- [39] C.K. Modi, S.H. Patel, M.N. Patel, *J. Therm. Anal. Calorim.* 87 (2007) 441–448.
- [40] M.E. El-Zaria, *Spectrochim. Acta A* 69 (2008) 216–221.
- [41] H.M. Parekh, P.K. Panchal, M.N. Patel, *J. Therm. Anal. Calorim.* 86 (2006) 803–807.